

## A novel synthesis of ditrimethylolpropane biphosphoramidate diethyleneamine as flame retardant and antistatic textiles

Wei Jiang\*, Jin-Feng Li\*, Zi-Yuan Li\*, Xiao-Yan Zhang\*\*, Fan-Long Jin<sup>\*,†</sup>, and Soo-Jin Park<sup>\*\*\*,†</sup>

\*Department of Polymer Materials, Jilin Institute of Chemical Technology, Jilin City 132022, P. R. China

\*\*Refinery of Jilin Petrochemical Company, Jilin City 132022, P. R. China

\*\*\*Department of Chemistry, Inha University, Incheon 22212, Korea

(Received 29 July 2020 • Revised 7 January 2021 • Accepted 26 January 2021)

**Abstract**—A novel phosphorous- and nitrogen-containing flame retardant, ditrimethylolpropane biphosphoramidate diethyleneamine (DBD), was synthesized. Its chemical structure is characterized by Fourier-transform infrared spectroscopy and <sup>1</sup>H nuclear magnetic resonance spectroscopy. The effect of DBD on the physical, mechanical, and antistatic properties, thermal stability, and flame retardancy of wool fabric was systematically investigated. Thermogravimetric analysis showed that the initial decomposition temperature of DBD was 165 °C and 243 °C under nitrogen and air atmosphere, respectively. Furthermore, after 30 washes, the treated wool fabric exhibited excellent wash durability and good antistatic properties. Vertical burning tests indicated that both the burning time and char length of the treated wool fabric were lower than those of the flame-retardant standard, leading to a B1 flame retardant rating for the treated wool fabric. Compared to untreated wool fabric, the limiting oxygen index value of treated wool fabric increased significantly from 25.7% to 34.7%.

Keywords: Flame Retardant, Wool Fabric, Thermal Stability, Antistatic Property, Limiting Oxygen Index

### INTRODUCTION

In recent years, three major synthetic materials have shown rapid development, as have their products, including plastic tubes, sheets, films, bottles, tires, shoes, and clothes. These materials are plastics, such as polypropylene (PP), polyvinyl chloride, epoxy resin, and phenolic resin, synthetic rubbers, such as styrene butadiene rubber, neoprene, and nitrile butadiene rubber, and synthetic fibers, such as nylon, polyester, and polyacrylonitrile. These polymeric materials are supplanting natural and traditional materials, including metal, cement, and wood, because they are energy-efficient, lightweight, and highly compatible with processing techniques [1-3]. Wool textiles are natural fibers widely used in floor carpeting, clothing, and suiting, with many advantages, such as high warmth, breathability, and some level of inherent stain resistance and flame retardancy [4-7]. Despite the inherent flame retardancy of wool due to its high nitrogen and sulfur content, it is still flammable. It will ignite when exposed to an open flame and it easily decomposes and burns at high temperature. Molten wool drips can ignite other combustibles, creating a serious fire hazard. Moreover, wool does not burn completely during combustion, releasing large amounts of CO<sub>2</sub> and CO and causing significant environmental pollution [8-10].

Wool is often subjected to flame-retardant treatment to improve its flame retardancy. A range of solution techniques such as coprecipitation, solvothermal methods, hydrothermal processing, and

sol-gel chemistry have been used for flame-retardant treatment of wool fabrics [11]. Among commonly used flame retarding agents, halogenated flame retardants have historically played an important role in improving flame retardancy. However, these flame retardants have many disadvantages, including the generation of copious amounts of toxic and corrosive gases during combustion [12-15]. Therefore, the development of halogen-free flame retardants, with low toxicity, low smoke, low environment impact, and good flame-retardant properties to replace existing agents, has become of growing interest worldwide.

Recently, various halogen-free flame retardants, such as phosphorus-, nitrogen-, and silicon-containing agents, have been developed and used to treat the surface of wool fibers [1618]. In addition, various inorganic nanoparticles, such as silver, titanium dioxide (TiO<sub>2</sub>), copper, and silica, have been used as finishing agents on wool surfaces to improve their flame retardant, antibacterial, and antistatic properties [19-21]. During combustion, phosphorus-containing flame retardants can release phosphoric acids that accelerate the char formation of wool, protecting the wool from heat transfer and reducing the formation of combustible volatiles [22]. Nitrogen-containing flame retardants produce incombustible gases upon heating, such as nitrogen or ammonia, which can form a protective barrier for wool against flame and heat, but also dilute the combustible species [23]. During burning, silicon-containing flame retardants form a stable heat-insulating carbon protective layer with creation of -Si-O- and -Si-C- bonds, which inhibits flammable products from diffusing into the flame and insulates the wool surface from heat [24].

Research on flame retardant treatments has shown promising results on improving the flame retardancy of wool fabric. Cheng et

<sup>†</sup>To whom correspondence should be addressed.

E-mail: jinfanlong@163.com, sjpark@inha.ac.kr

Copyright by The Korean Institute of Chemical Engineers.

al. [9] prepared a water-soluble polyelectrolyte complex using phytic acid (PA) and polyethyleneimine (PEI) to improve the flame retardancy of wool fabric. Their results indicated that wool fabric treated with a polyelectrolyte complex consisting of 15% PA and 15% PEI was still able to self-extinguish after ten washing cycles. In another example, Cheng et al. [7] treated wool fabric using a PA/chitosan polyelectrolyte complex. Results showed that one coating deposition with a polyelectrolyte complex consisting of 10% PA and 2% chitosan effectively prevented the burning of wool fabric. Cheng et al. [8] also treated wool fabric using PA, TiO<sub>2</sub> nanoparticles, and 1,2,3,4-butanetetracarboxylic acid (BTCA). Their results showed that the PA/TiO<sub>2</sub>/BTCA system endowed wool fabric with excellent flame retardancy and washing durability. Kaynak et al. [25] treated wool and wool/nylon-blended fibers using a phosphorus- and sulfur-based flame retardant. Their results indicated that heat release was effectively reduced with this treatment. Mathur et al. [26] treated wool using sulfamic acid, a nitrogen- and sulfur-containing compound, as a flame retardant. Results showed that the limiting oxygen index (LOI) of the wool was increased and char formation with decreased char length was facilitated after the flame retardant treatment. Cheng et al. [11] synthesized a reactive PA-based flame retardant and used it to prepare a flame retardant-functionalized wool fabric. Results showed that wool fabric treated with 0.14 M flame retardant exhibited self-extinguishing performance even after 20 washing cycles. Shan et al. [27] synthesized a phosphorus- and silicon-containing flame-retardant monomer and used it to treat wool fabric. Results showed improved thermal sta-

bility and flame retardancy of the wool fabric, the latest being retained even after 15 washing cycles. Li et al. [28] synthesized flame-retardant antistatic phosphorus-containing copolymers and applied them to PP. Their results showed that the flame-retardant effect of the copolymers on PP was unsatisfactory. When the copolymer content in PP was 20 wt%, PP composites demonstrated good antistatic effects. Despite flourishing research in the area, there have been no reports of phosphorus-containing compounds being used as flame retardant and antistatic agents for wool fabric.

In this study, a novel phosphorus- and nitrogen-containing flame retardant agent, ditrimethylolpropane biphosphoramidate diethyleneamine (DBD), is synthesized and used as a flame retardant and antistatic agent for wool fabric. The chemical structure and thermal properties of DBD are characterized by Fourier transform infrared spectroscopy (FT-IR), <sup>1</sup>H nuclear magnetic resonance spectroscopy (NMR), and thermogravimetric analysis (TGA). The influence of added DBD on the thermal stability, physicochemical, antistatic, and flame-retardant properties of wool fabric is investigated.

## EXPERIMENTAL

### 1. Materials

Ditrimethylolpropane, phosphoryl chloride (POCl<sub>3</sub>), and ethylenediamine were supplied as raw materials from Jihua branch of Petrochina, Jihua Group Corporation, and Shandong Haihua Group Co. Ltd., respectively. 1,4-Dioxane was used as a solvent and pur-

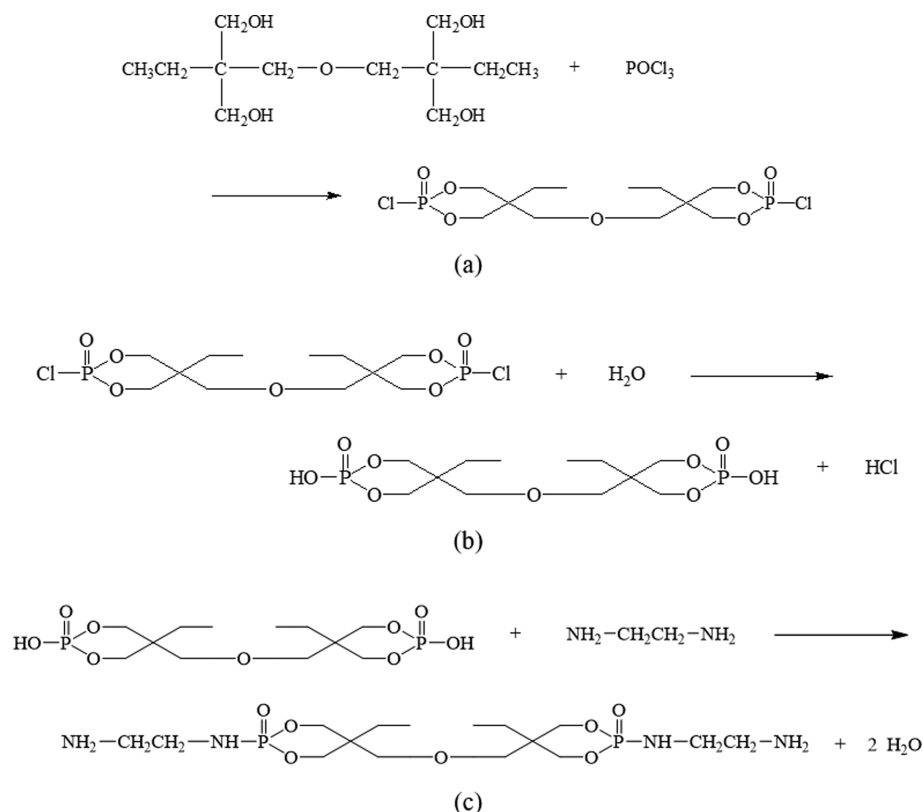


Fig. 1. Schematic outline for the synthesis of DBD.

chased from Shenyang Xinxi Reagent Factory. All chemicals were used as received and without further purification. The wool fabric used in this study was woven scoured fabric, with a weight of 220 g/m<sup>2</sup> and a fiber diameter of 38 μm.

## 2. Synthesis of DBD

The schematic in Fig. 1 outlines the synthesis of the developed phosphorus- and nitrogen-containing flame retardant, DBD, involving three steps: esterification, hydrolysis, and neutralization, explained in detail below.

**Esterification:** Ditrtrimethylolpropane (25 g, 0.1 mol), POCl<sub>3</sub> (38.3 g, 0.25 mol), and 1,4-dioxane (40 mL) were mixed in a 250 mL glass flask equipped with a mechanical stirrer, a thermometer, and a reflux condenser. The mixture was gradually heated to 50 °C and allowed to react for 5 h. After the reaction, the 1,4-dioxane and unreacted POCl<sub>3</sub> were removed by distillation under vacuum, leading to a highly viscous, light yellow liquid, namely ditrimethylolpropane diphosphorus chloride (DDC). Fig. 2(a) shows a digital image of DDC.

**Hydrolysis:** DDC (41 g, 0.1 mol) was dissolved in 1,4-dioxane (8 mL), followed by addition of distilled water (4.5 g, 0.25 mol) to the solution. The mixture was gradually heated to 72 °C and allowed to react for 1.5 h. The 1,4-dioxane was subsequently removed by distillation and a highly viscous, light yellow liquid was obtained, namely ditrimethylolpropane diphosphate ester (DDE). Fig. 2(b) shows a digital image of DDE.

**Neutralization:** DDE (37 g, 0.1 mol) was dissolved in 1,4-dioxane (10 mL), followed by addition of ethylenediamine (13.2 g, 0.22 mol) to the solution. The mixture was gradually heated to 75 °C and allowed to react for 3 h. Then, 1,4-dioxane and unreacted ethylenediamine were removed by distillation under vacuum, yielding a

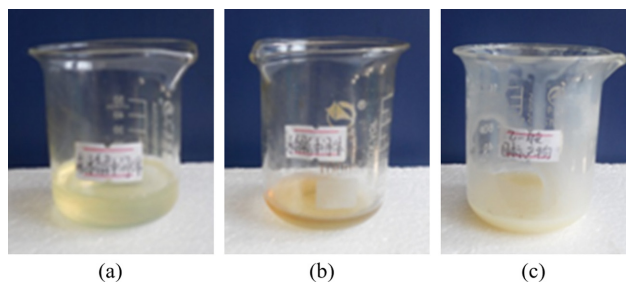


Fig. 2. Digital images of DDC (a), DDE (b), and DBD (c).

highly viscous, light yellow liquid, DBD (yield: 91.1%), as shown in Fig. 2(c).

## 3. Preparation of DBD-Treated Wool Fabric

A schematic diagram of the DBD treatment process for wool fabric is shown in Fig. 3. DBD (200 g) was added to distilled water (800 mL) and stirred at 30 °C for 20 min. Then, three pieces of wool fabric with various dimensions were immersed in the DBD solution at 60 °C for 20 min. The wetness pickup was controlled by adjusting the distance between rolling wheels. After two rounds of immersion and rolling that enabled a wetness pickup of 70-90%, the DBD-treated wool fabric was dried at 80 °C for 10 min and 160 °C for 3 min. Digital images of the wool fabric before and after DBD treatment are shown in Fig. 4.

## 4. Characterization

### 4-1. Structural Characterization

FT-IR spectroscopy was performed with a spectrometer (Bio-Rad Co., Digilab FTS-165) using KBr pellets. <sup>1</sup>H NMR (400 MHz) spectra were obtained using a Bruker 400 M spectrometer and

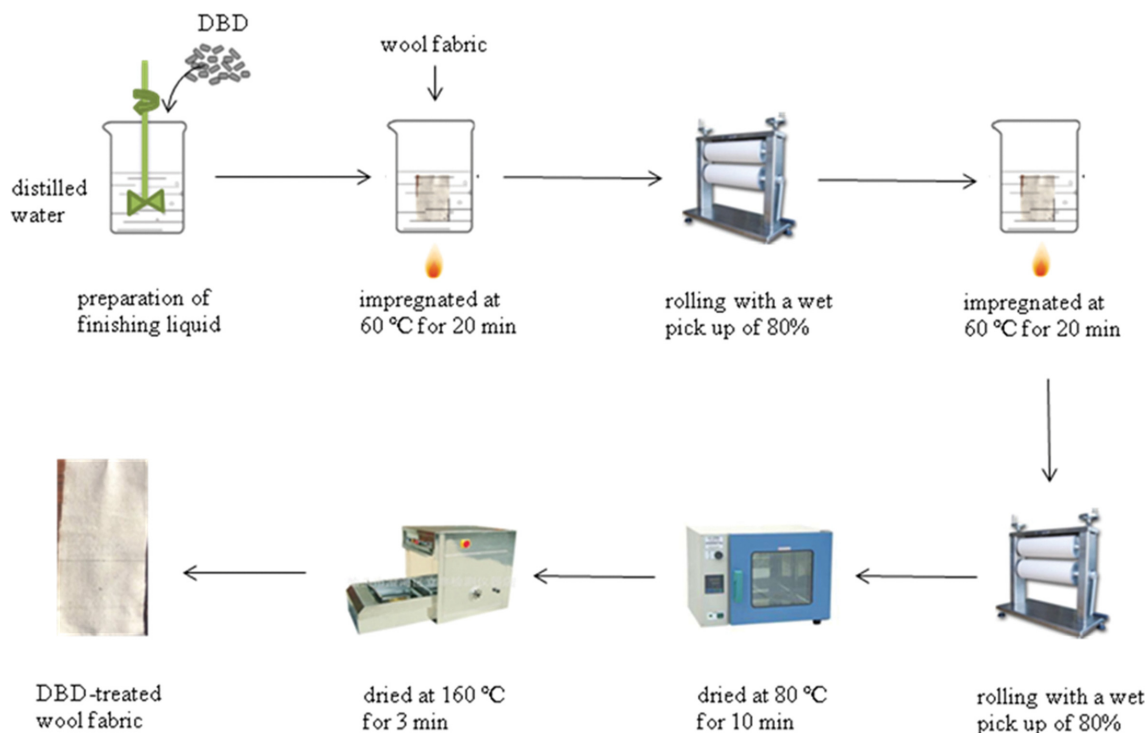


Fig. 3. Schematic diagram of DBD treatment process for wool fabric.

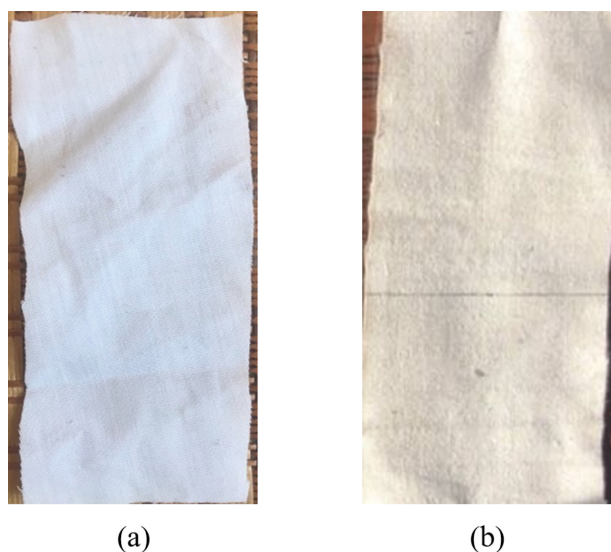


Fig. 4. Digital images of untreated (a) and DBD-treated wool fabrics (b).

$\text{CDCl}_3$ ,

#### 4-2. Weight Gain

The wool fabric was dried at  $80^\circ\text{C}$  for 10 min and  $160^\circ\text{C}$  for 3 min and weighed as quickly as possible thereafter. The weight gain of the treated wool fabric was calculated according to the following equation:

$$\text{Weight gain (\%)} = (W_2 - W_1) / W_1 \times 100 \quad (1)$$

where  $W_1$  and  $W_2$  are the weights of the wool fabric before and after treatment, respectively.

#### 4-3. Breaking Strength Test

The breaking strength of wool fabric was determined according to the strip method for the determination of tensile properties and breaking strength of fabrics (GB/T 3923.1-1997) using an electronic fabric strength machine (YG026T). The sheet dimensions were  $5.5\text{ mm} \times 30\text{ mm}$ , and the tensile speed and distance between the two clamps were  $50\text{ mm/min}$  and  $200\text{ mm}$ , respectively. The reported breaking strength was determined by averaging the results of five repeated experiments.

#### 4-4. Whiteness Test

The whiteness of wool fabric was measured according to the fabric whiteness determination method (GB/T 7973-2003) using a whiteness meter (WBS-1). The reported whiteness was determined by averaging the results of five repeated experiments.

#### 4-5. Wash Durability Test

The wash durability of wool fabric was determined according to the test method for fabric washing fastness (GB/T 3921.1-5) using a color fastness to washing tester (SW-12A). The sheet dimensions were  $10\text{ mm} \times 40\text{ mm}$ . The environmental temperature and relative humidity were  $20 \pm 2^\circ\text{C}$  and  $35 \pm 5\%$ , respectively. The reported wash durability was determined by averaging the results of three repeated experiments.

#### 4-6. Antistatic Properties

Following the determination of static voltage half-life of textile electrostatic properties (FZ/T 01042-1996), the electrostatic half-life

was measured to determine the antistatic properties of wool fabric using a fabric induction-type electrostatic tester (M401). The sample sheet dimensions were  $10\text{ mm} \times 40\text{ mm}$ , the distance between the needle electrode and the sample was  $20\text{ mm}$ , the distance between the test probe and the sample was  $15\text{ mm}$ , and the voltage was  $10\text{ kV}$ . The reported half-life was determined by averaging the results of three repeated experiments.

#### 4-7. Thermal Stability

The thermal and thermo-oxidative stability of DBD and wool fabric were investigated using a thermogravimetric analyzer (TA Instruments, Q50) using a temperature range of  $30^\circ\text{C}$  to  $600^\circ\text{C}$  at a heating rate of  $10^\circ\text{C/min}$  under nitrogen and air atmospheres (gas flow was  $30\text{ mL/min}$ ). The reported thermal properties were determined by averaging the results of two repeated experiments.

#### 4-8. Morphology

The surface morphology of wool fabric was investigated using high-resolution scanning electron microscopy (HR-SEM; Hitachi, SU 8010). An energy-dispersive X-Ray (EDX) spectrometer coupled to the SEM was used to check for presence of phosphorus.

#### 4-9. Vertical Combustion Test

Vertical combustion tests of wool fabric were carried out according to the textile-determination of burning characteristics-vertical test (GB/T 5455-1997) using a fabric flame retardant tester (Wenzhou Fangyuan Instrument Co. Ltd., YGB815A). The reported burning time and char length were determined by averaging the results of three repeated experiments.

#### 4-10. LOI Test

The LOI values of wool fabric were determined at room temperature using an oxygen index instrument (Qingdao Shanfang Instrument Co. Ltd., ZR-01) according to the determination of combustion performance of textiles-determination of oxygen index (GB/T 5454-1997). The reported LOI was determined by averaging the results of three repeated experiments.

#### 4-11. Cone Calorimetry Test

The heat release rate (HRR) and smoke production rate (SPR) were measured by a cone calorimeter (JCZ-2, Nanjing Analytical Instrument Factory Co., Ltd.) according to GB/T 33618-2017 under a heat flux of  $35\text{ kW/m}^2$ . The sample sheet dimensions were  $100\text{ mm} \times 100\text{ mm}$ .

## RESULTS AND DISCUSSION

### 1. Synthesis of DBD

The chemical structure of DBD was characterized by FT-IR and  $^1\text{H}$  NMR. The FT-IR spectrum of DBD, shown in Fig. 5(a), indicates that DBD exhibits a broad absorption around  $3,370\text{ cm}^{-1}$  that can be assigned to the N-H stretching vibration. The absorption peaks at  $2,967\text{ cm}^{-1}$  and  $1,884\text{ cm}^{-1}$  indicate the presence of  $\text{CH}_3$  groups, while the absorption peak at  $2,930\text{ cm}^{-1}$  reveals the presence of  $\text{CH}_2$  groups. The characteristic absorption peaks at  $1,378\text{ cm}^{-1}$  and  $1,054\text{ cm}^{-1}$  are attributed to the P=O and P-O-C groups, respectively [29,30].

The  $^1\text{H}$  NMR spectrum of DBD ( $\text{CDCl}_3$ ), shown in Fig. 5(b), reveals peaks at  $\delta = 3.61\text{--}3.73\text{ ppm}$  ( $\text{CH}_2\text{-O}$ ),  $2.252\text{--}3.1\text{ ppm}$  ( $\text{NH}$ ),  $1.51\text{--}1.66\text{ ppm}$  ( $\text{NH}_2$ ),  $1.151\text{--}1.33\text{ ppm}$  ( $\text{CH}_2$ ), and  $0.77\text{--}0.88\text{ ppm}$  ( $\text{CH}_3$ ) [31,32].

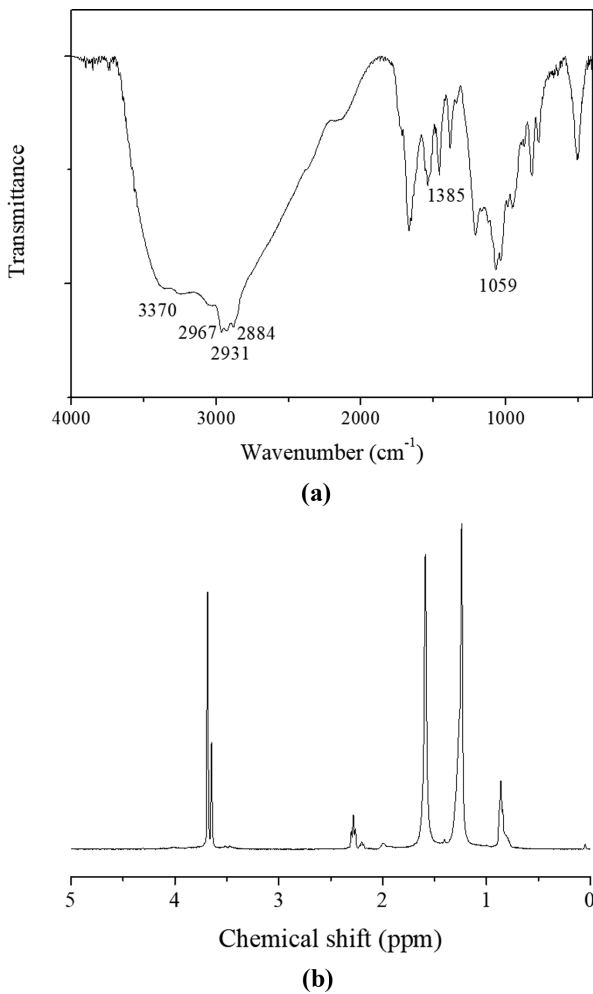


Fig. 5. FT-IR (a) and <sup>1</sup>H NMR (b) spectra of DBD.

Table 1. Weight gain of DBD-treated wool fabric as a function of DBD concentration

Concentration (g/L)	100	200	300	400
Weight gain (%)	5.4	12.1	15.1	20.6

2. DBD Treatment of Wool Fabric

Wool fabric was treated using various DBD concentrations. Table 1 shows the weight gain of wool fabric treated with different DBD concentrations. The weight gain of DBD-treated wool fabric increased from 5.4% to 20.6% with increasing DBD concentration from 100 g/L to 400 g/L.

3. Physicomechanical Properties

The breaking strengths of DBD-treated wool fabric in the warp and weft directions as a function of curing time are shown in Fig. 6. It can be seen that the breaking strength of treated wool fabric in the warp direction increases with increasing curing time up to 90 s, after which it decreases. Similarly, the breaking strength of treated wool fabric in the weft direction also shows a maximum value at a curing time of 90 s. The breaking strength of treated wool fabric in the warp and weft directions, at a baking time of 90 s, was 368.8 N and 368.8 N, respectively, lower than that of untreated wool

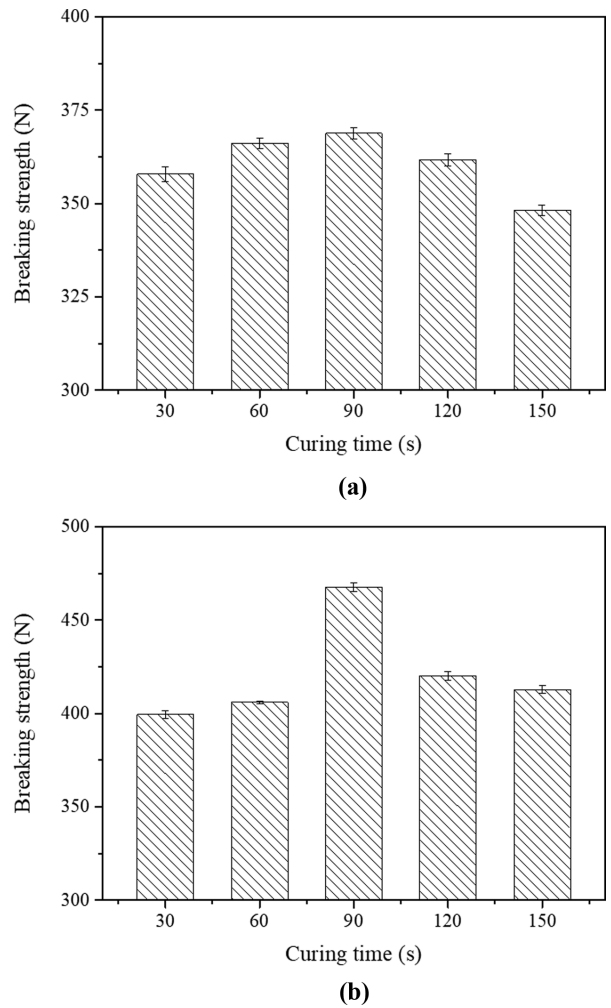


Fig. 6. Breaking strength of DBD-treated wool fabric as a function of curing time: (a) Warp direction; (b) weft direction.

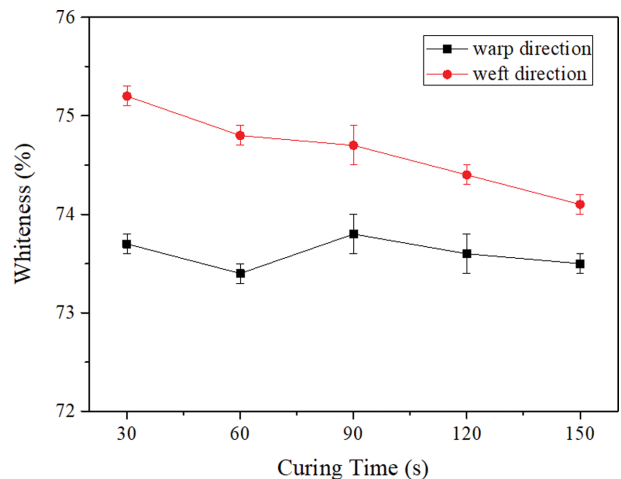


Fig. 7. Whiteness of DBD-treated wool fabric as a function of curing time.

fabric by 14% and 11%, respectively. The untreated wool fabric had a breaking strength of 432.7 N in the warp direction and 529.4 N

in the weft direction. These results suggest that the DBD treatment affects the breaking strength of wool fabric [33,34]. This can be explained by the highly acidic pH of DBD, about 2, which when applied in high concentration (300 g/L) on the wool fabric and cured at a high temperature (160 °C), resulted in reduced breaking strength of the wool fabric.

The whiteness of wool fabric in the warp and weft directions as a function of baking time is shown in Fig. 7. The whiteness of treated wool fabric decreased slightly in both directions with increasing curing time, and it was measured at 73.8 and 74.7 in the warp and weft directions, respectively, at a curing time of 90 s. This was 0.4% and 1.2% lower than that of untreated wool fabric, which had a whiteness of 74.1 in the warp direction and 75.6 in the weft direction. These results, therefore, indicate that treatment with DBD

slightly affects the whiteness of wool fabric [11,35]. Note that, despite the slight decrease in whiteness, the whiteness of all samples treated with DBD still fell within the requirement of 67-75 whiteness for white fabrics. Generally, the whiteness of fabrics can be measured irrespectively of warp and weft directions, since it is mainly related to their density. In this case, the number of yarns in the warp direction was greater than that in the weft direction, which caused a difference in density between the two directions. Therefore, the whiteness of the warp direction was higher than that of the weft direction, because the light source was reflected differently by the fabric. According to both the breaking strength and whiteness tests, the optimal curing time was 90 s.

#### 4. Antistatic Properties

Table 2 shows the electrostatic half-lives of wool fabric in the

**Table 2. Half-life of untreated and DBD-treated wool fabrics**

Sample	Number of wash cycles (times)	Warp half-life (s)	Weft half-life (s)
Untreated wool fabric	0	43.5±0.4	42.6±0.4
DBD-treated wool fabric	10	5.9±0.2	3.6±0.1
DBD-treated wool fabric	20	7.4±0.1	7.2±0.1
DBD-treated wool fabric	30	9.9±0.2	7.5±0.1

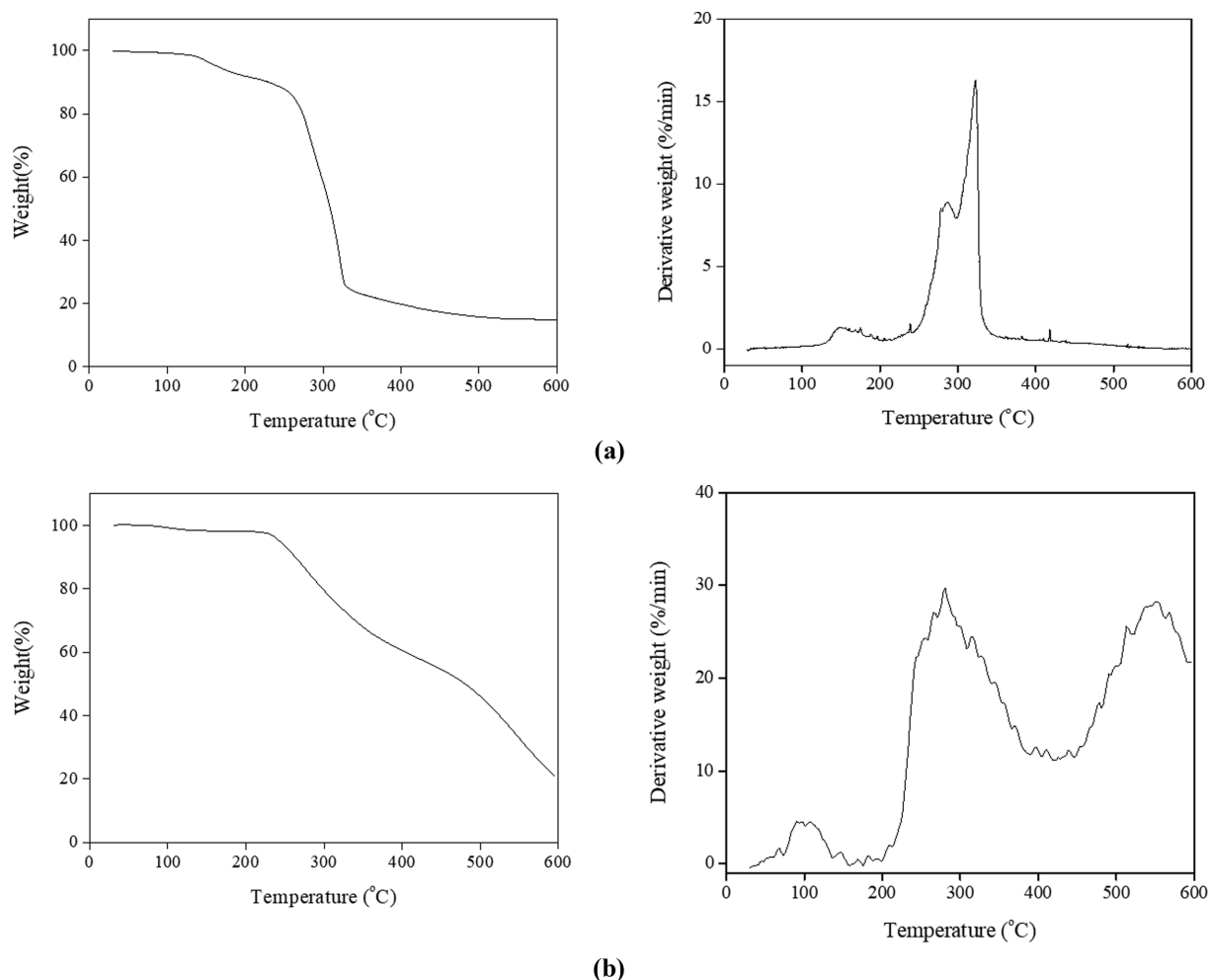


**Fig. 8. TGA and DTG curves of DBD in nitrogen (a) and air atmosphere (b).**

warp and weft directions as a function of the number of wash cycles. Untreated wool fabric had a half-life of 43.5 s in the warp direction and 42.6 s in the weft direction, both much higher than the maximum requirement of 15 s for durable antistatic textiles as specified in the national standard. Thus, untreated wool fabric does not exhibit any antistatic properties [36]. When subjected to DBD treatment, the half-life of treated wool fabric gradually increased with an increasing number of wash cycles, indicating that the antistatic properties of treated wool fabric decreased after washing.

The half-lives of treated wool fabric in the warp and weft directions after 30 washes were 9.9 s and 7.9 s, respectively, much lower than the 15 s requirement for durable antistatic textiles as mentioned earlier. This can be explained by the presence of the amine group in DBD, which is a polar hydrophilic group that can absorb moisture, resulting in a decrease in surface electrical resistivity. Decreased surface electrical resistivity can lead to a decrease in static charge accumulation and an increase in antistatic property [37].

The aforementioned results indicate that treated wool fabric had higher wash durability and antistatic property than untreated wool fabric.

### 5. Thermal Properties

TGA and differential thermal analysis (DTA) were used to investigate the thermal properties of DBD and wool fabric. The weight loss and derivative weight loss for DBD as a function of temperature under nitrogen and air atmospheres are shown in Fig. 8. Thermal stability factors, such as the initial decomposition temperature (the temperature of 5% weight loss,  $T_{5\%}$ ), temperature at maximum weight loss rate ( $T_{max}$ ), and char residue at 600 °C, were extracted from the TGA and DTA thermograms [38,39], with results summarized in Table 3.

It was found that DBD started decomposing at 165 °C and 243 °C under nitrogen and air atmosphere, respectively. In addition, the char residue at 600 °C was 20.8% under air atmosphere, which was higher than that under nitrogen atmosphere (14.8%). The DTA

**Table 3. Thermal stability factors of DBD obtained from TGA and DTA thermograms**

Atmosphere	$T_{5\%}$ (°C)	$T_{max1}$ (°C)	$T_{max2}$ (°C)	$T_{max3}$ (°C)	Char at 600 °C (wt%)
Nitrogen	165	150	287	322	14.8
Air	243	100	280	552	20.8

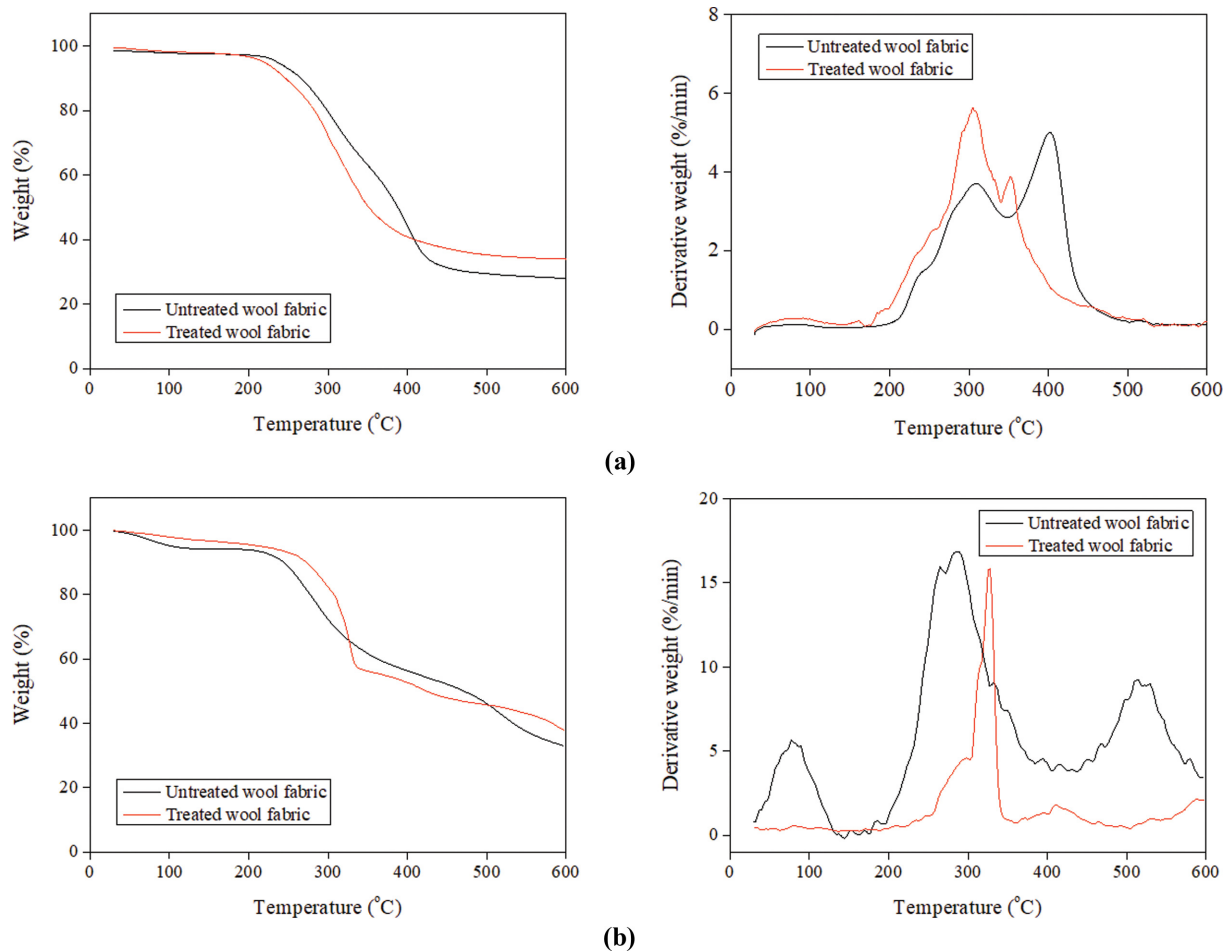


**Fig. 9. TGA and DTG curves of untreated and DBD-treated wool fabric in nitrogen (a) and air atmosphere (b).**

**Table 4. Thermal stability factors of untreated and DBD-treated wool fabrics obtained from TGA and DTA thermograms**

Sample	Atmosphere	T <sub>5%</sub> (°C)	T <sub>max1</sub> (°C)	T <sub>max2</sub> (°C)	T <sub>max3</sub> (°C)	Char at 600 °C (wt%)
Untreated wool fabric	Nitrogen	239	308	401	-	28.0
DBD-treated wool fabric	Nitrogen	220	305	352	-	34.0
Untreated wool fabric	Air	103	79	286	513	33.0
DBD-treated wool fabric	Air	214	327	-	-	37.8

results reveal that DBD had a minor weight loss stage at 150 °C and a major weight loss stage at 287–322 °C under nitrogen atmosphere. Under air atmosphere, DBD had a minor weight loss stage at 100 °C and a major weight loss stage at 280–552 °C. These results are attributed to the scission of the phosphate ester bonds and the formation of a phosphorus-rich char layer [40].

The weight loss and derivative weight loss as a function of temperature for the untreated and DBD-treated wool fabrics under nitrogen and air atmosphere are shown in Fig. 9, and the corresponding thermal stability factors are listed in Table 4. The initial decomposition temperature of untreated wool fabric was found to be 239 °C under nitrogen and 103 °C under air atmosphere. Two maximum weight loss temperatures at 308 °C and 401 °C under nitrogen atmosphere were observed. In contrast, under air atmosphere, three maximum weight loss temperatures were observed, at 79 °C, 286 °C, and 513 °C were observed. The char residues of the untreated wool fabric at 600 °C were 28% under nitrogen and 33% under air atmosphere [41].

The initial decomposition temperature of DBD-treated wool

fabric was 220 °C under nitrogen atmosphere and 214 °C under air atmosphere, which could be attributed to the decomposition of DBD and the formation of phosphoric acid or polyphosphate. The DTA results indicate that two maximum weight loss temperatures, at 313 °C and 352 °C, were observed under nitrogen atmosphere, in contrast to the single maximum weight loss temperature, at 327 °C, observed under air atmosphere. The char residue of treated wool fabric at 600 °C was 34% under nitrogen and 37.8% under air atmosphere, both higher than those of untreated wool fabric. These results indicate that DBD decomposed and produced phosphorus-rich char, promoting the esterification and carbonization of wool fabric, which effectively protected the wool fabric [42–44].

## 6. Morphology

To investigate the morphology of the wool fabric before and after the flame-retardant treatment and to assess the extent of the presence of the flame retardant, SEM-EDX analysis was carried out. SEM images of the untreated and DBD-treated wool fabrics at different magnifications are shown in Fig. 10. As shown in Fig. 10(a), (b), the untreated wool fabric exhibited a smooth surface. In

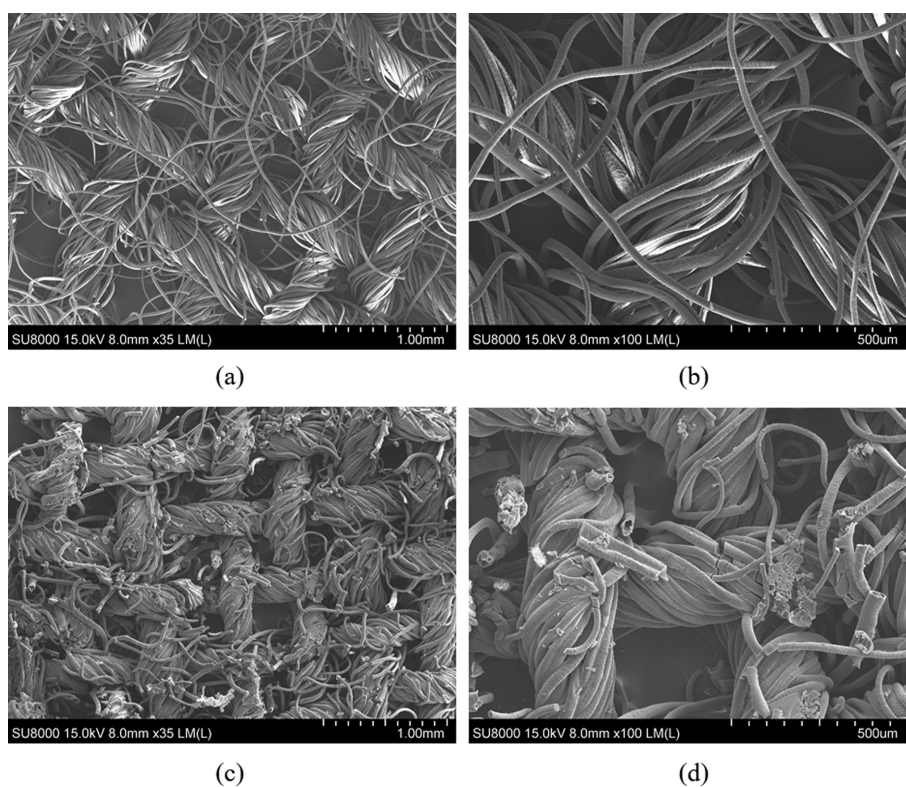


**Fig. 10. SEM images of untreated (a), (b) and DBD-treated wool fabrics (c), (d) at different magnification.**

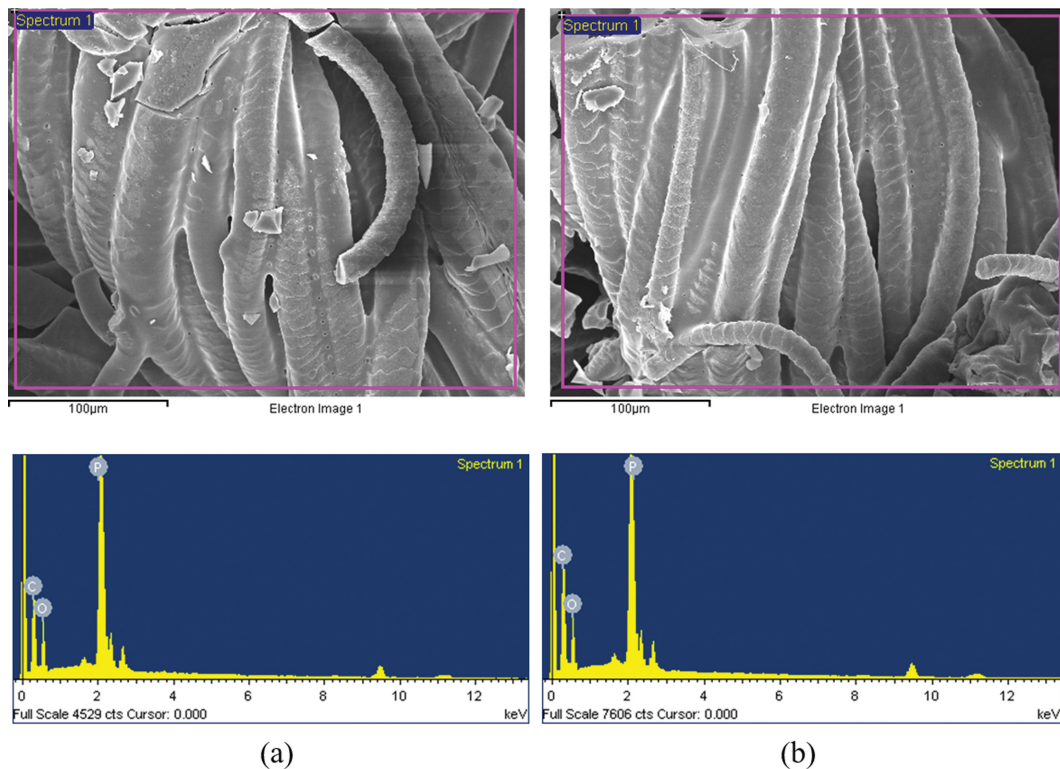


Fig. 11. EDX mapping of DBD-treated wool fabrics before (a) and after burning test (b).

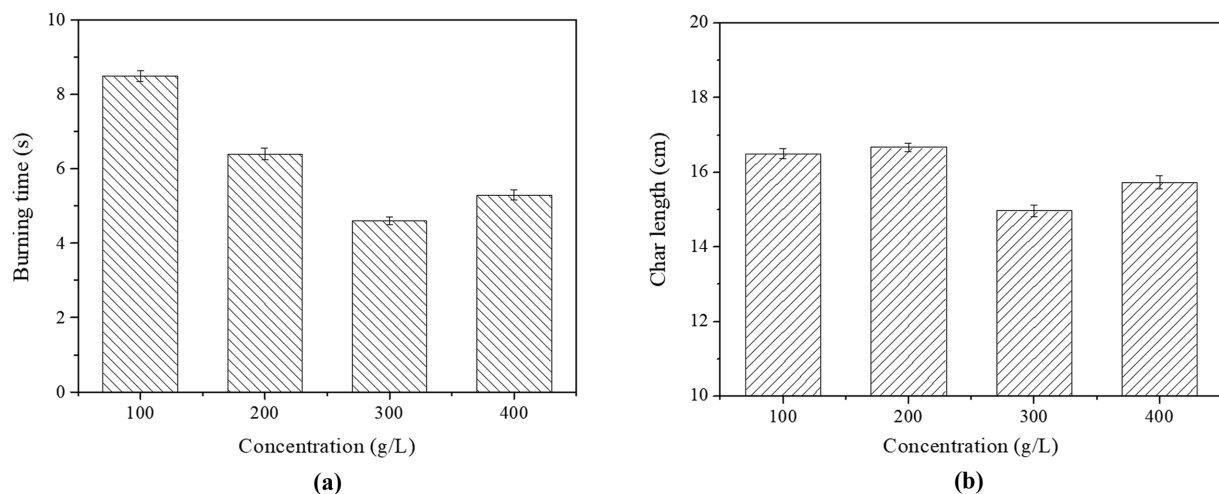


Fig. 12. Burning time (a) and char length (b) of DBD-treated wool fabric as a function of DBD concentration.

contrast, the DBD-treated wool fabric showed presence of micro-sized DBD particles on the fabric surface, as shown in Fig. 10(c), (d). The EDX mapping of DBD-treated wool fabric revealed that the C, O, and P elements were present on the DBD-treated wool fabric at 65.81, 26.37, and 7.82%, respectively, as shown in Fig. 11(a). These results confirm that DBD was successfully coated onto the wool fabric surface.

### 7. Flame-retardant Properties

The flame-retardancy of DBD-treated wool fabric was determined by vertical burning, LOI, and cone calorimetry tests. The burning time and char length of wool fabric as a function of DBD

concentration are shown in Fig. 12. It was found that both the burning time and char length of treated wool fabric decreased with increasing DBD concentration up to 300 g/L, after which both parameters increased. Thus, according to the vertical burning tests, the optimal DBD concentration was 300 g/L.

The burning time and char length of untreated wool fabric was 17.4 s and 25.2 cm, respectively, which indicates that untreated wool fabric is considered flammable. In contrast, the burning time and char length of wool fabric treated with a DBD solution of 300 g/L concentration was 4.6 s and 14.9 cm, respectively, values that satisfy the B1 level requirement for flame-retardant textiles. The

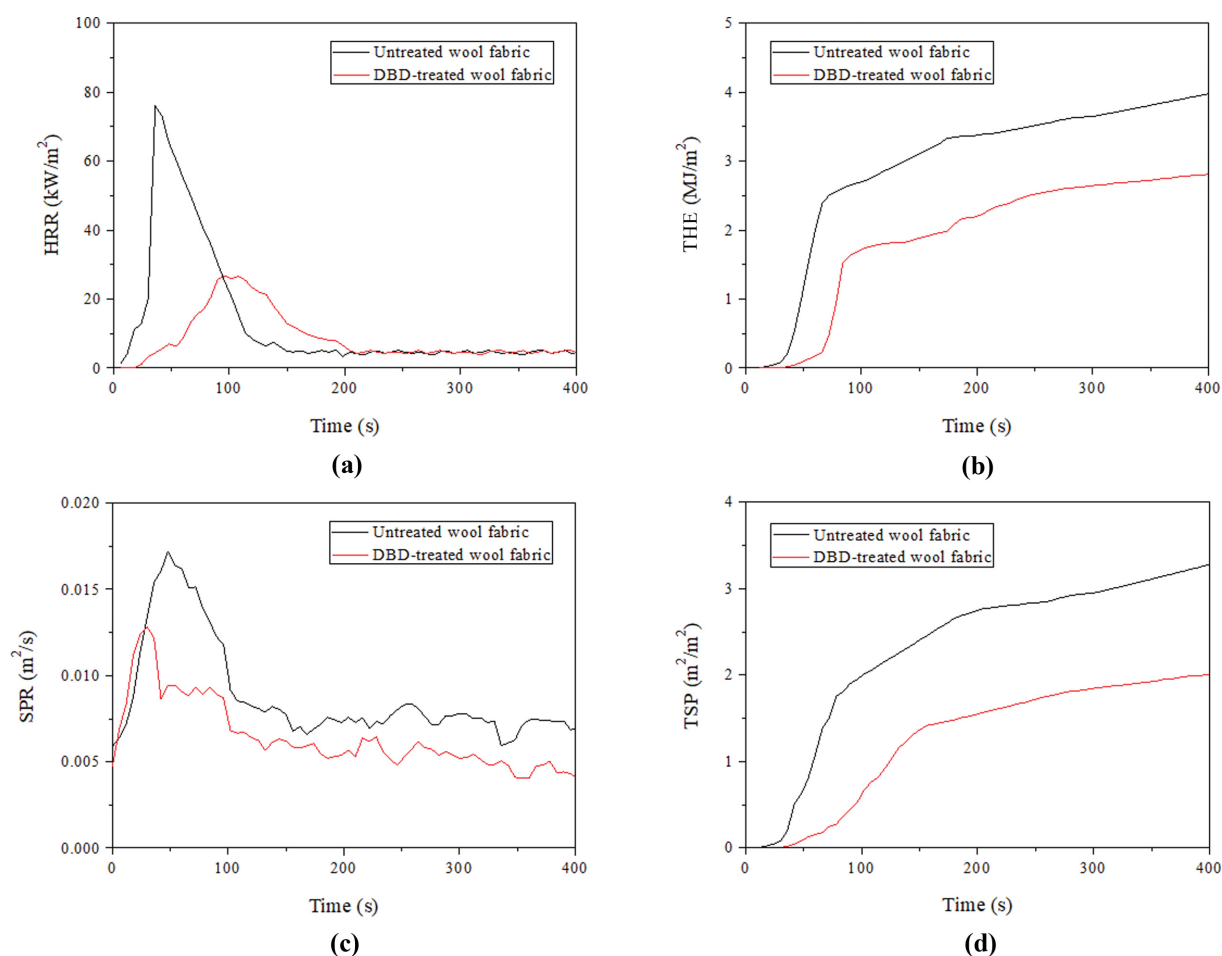


Fig. 13. HRR (a), THE (b), SPR (c), and TSP (d) curves of untreated and DBD-treated wool fabrics.

Table 5. THE, PHRR, and AV-MLR of untreated and DBD-treated wool fabrics

Sample	THE (MJ/m <sup>2</sup> )	PHRR (kW/m <sup>2</sup> )	AV-MLR (g/s)
Untreated wool fabrics	3.99	76.45	0.014
DBD-treated wool fabrics	2.82	26.57	0.012

char length of wool fabric treated with a 300 g/L DBD solution is reduced by 40% compared to untreated pure wool fabric. This reduction may be attributed to the formation of a phosphorus-rich char layer, derived from the decomposition of DBD during burning. This layer acts as a barrier against the release of flammable pyrolysis products generated during the burning of wool fabric [45–47]. These results show that the DBD treatment significantly improved the flame-retardancy of wool fabric.

LOI is defined as the minimum oxygen concentration required to support the combustion of a material in a mixture of oxygen and nitrogen gas under specified conditions. A high LOI value means the material is difficult to combust, whereas a low LOI value implies easy combustion. The LOI value of untreated wool fabric was found to be 25.7%, indicating that untreated wool fabric is a slow-burning material. In contrast, the LOI value of DBD-treated wool fabric was 34.7%, higher than the 28% LOI standard value

for a flame-retardant, suggesting that the DBD-treated wool fabric exhibits high flame retardancy [48,49].

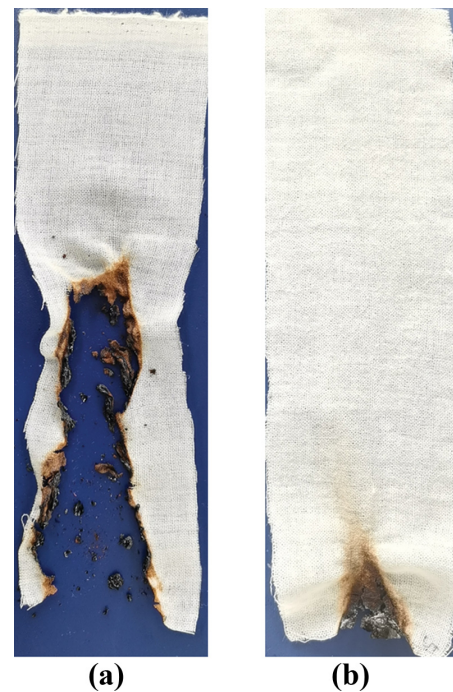
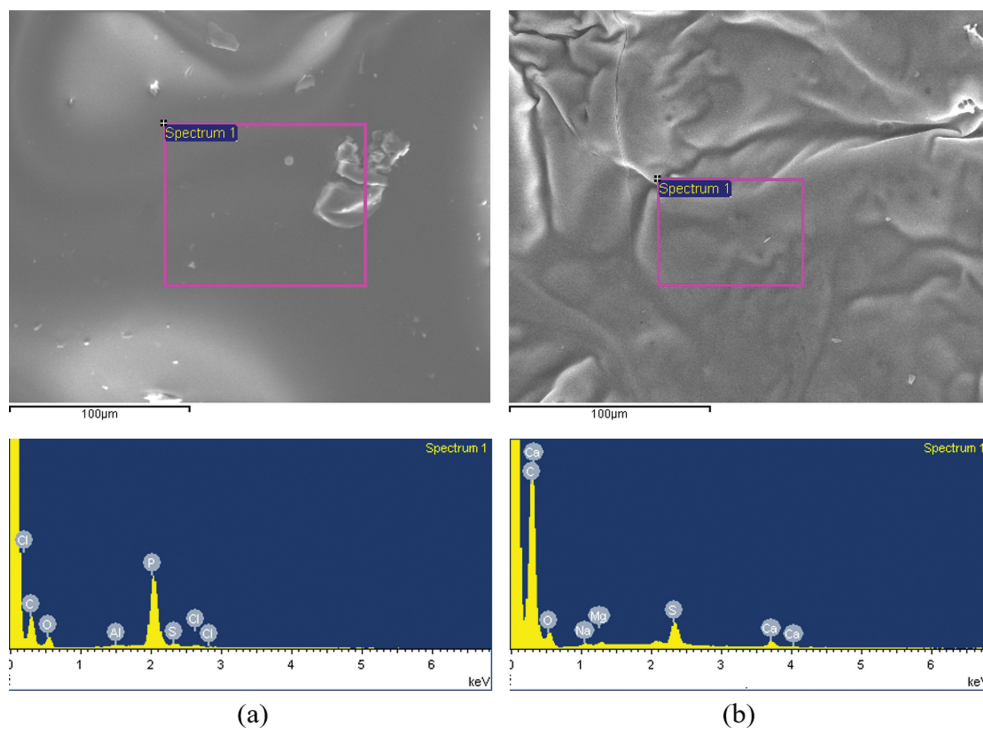
The flame retardancy of DBD-treated wool fabric was further investigated through a cone calorimetry test. The HRR and total heat release (THR) curves of untreated and DBD-treated wool fabrics are shown in Figs. 13(a) and (b). The THR, peak rate of heat release (PHRR), and average mass loss rate (AV-MLR) data were obtained by integrating the HRR and THR curves, and the results are listed in Table 5. Compared with the untreated wool fabric, THR and PHRR of DBD-treated wool fabric decreased significantly from 3.99 MJ/m<sup>2</sup> and 76.45 kW/m<sup>2</sup> to 2.82 MJ/m<sup>2</sup> and 26.57 kW/m<sup>2</sup>, respectively. This decrease indicated that DBD as flame retardant reduced dramatically the combustion density of wool fabric during burning, hence endowed wool fabric with outstanding flame retardancy [50]. The AV-MLR value of wool fabrics before and after DBD-treatment did not change significantly.

**Table 6. TSP, PSPR, and SmkFct of untreated and DBD-treated wool fabrics**

Sample	TSP ( $\text{m}^2/\text{m}^2$ )	PRSP ( $\text{m}^2/\text{s}$ )	SmkFct ( $\text{kW}/\text{m}^2$ )
Untreated wool fabrics	3.29	0.017	250.37
DBD-treated wool fabrics	2.02	0.013	53.97

The SPR and total smoke production (TSP) curves of untreated and DBD-treated wool fabrics are shown in Figs. 13(c) and (d). The TSR and peak rate of smoke production (PRSP) value were obtained by integrating the SPR and TSP curves, and the results are listed in Table 6. Compared to the untreated wool fabric, the TSP and PRSP of DBD-treated wool fabric decreased significantly, from  $3.29 \text{ m}^2/\text{m}^2$  and  $0.017 \text{ m}^2/\text{s}$  to  $2.02 \text{ m}^2/\text{m}^2$  and  $0.013 \text{ m}^2/\text{s}$  respectively. This result can be attributed to DBD decomposing at a relatively low temperature and accelerating the formation of a phosphorus-rich char layer, which can reduce the amount of smoke released [51]. Smoke factor (SmkFct), which is defined as the product of PHRR and TSP, is proposed as a good indicator of smoke produced from materials burning in a real fire. The SmkFct value of DBD-treated wool fabric ( $53.97 \text{ kW}/\text{m}^2$ ) was found much lower than that of untreated wool fabric ( $250.37 \text{ kW}/\text{m}^2$ ), indicating that the DBD-treated wool fabric is less likely to burn completely in a fire and produces less smoke when burning [25].

Digital images of untreated and DBD-treated wool fabric after the vertical burning tests are shown in Fig. 14. As shown in Fig. 14(a), untreated wool fabric burned quickly after ignition, leading to thorough damage [52]. In contrast, as shown in Fig. 14(b), the DBD-treated wool fabric showed a significantly reduced burning rate and formed a relatively complete char residue [53]. The EDX mapping of DBD-treated wool fabric after the vertical burning test

**Fig. 14. Digital images of untreated (a) and DBD-treated wool fabrics (b) after vertical combustion tests.****Fig. 15. EDX mapping of untreated (a) and DBD-treated wool fabrics (b) after cone calorimetry test.**

is shown in Fig. 11(b), revealing the presence of C, O, and P elements on the DBD-treated wool fabric at a percentage of 68.86%, 24.78%, and 6.35% respectively.

The EDX mapping of untreated and DBD-treated wool fabrics after cone calorimetry test is shown in Fig. 15, revealing the presence of C and O elements of untreated wool fabric at a percentage of 82.42% and 15.63%, respectively. The percentage of C, O, and P elements in DBD-treated wool fabric was 67.95%, 23.68%, and 7.66%, respectively, results consistent with the EDX results of wool fabric after the vertical burning test.

## CONCLUSIONS

A novel flame retardant, DBD, was synthesized and its chemical structure was characterized by FT-IR and <sup>1</sup>H NMR. Optimal flame-retardant properties of DBD-treated wool fabric were obtained at a DBD concentration and baking time of 300 g/L and 90 s, respectively. The treated wool fabric exhibited high wash durability and antistatic properties even after 30 washes. The initial decomposition temperature of DBD was found to be 165 °C and 243 °C under nitrogen and air atmosphere, respectively, which meets the processing temperature requirements for most products. DBD treatment significantly decreased the burning time and char length of wool fabric and increased the LOI value of wool fabric from 25.7% to 34.7%, indicating that DBD conferred excellent flame-retardancy. SEM results showed that the DBD-treated wool fabric formed a char residue and exhibited a significant decrease in char length compared to that of untreated wool fabric. This study demonstrates that DBD is a good flame retardant and antistatic agent for wool fabric.

## ACKNOWLEDGEMENTS

This work was supported by the Technology Innovation Program (or Industrial Strategic Technology Development Program-Development of technology on materials and components) (20010106, Adhesives with low water permeability and low out-gassing) funded By the Ministry of Trade, Industry & Energy (MOTIE, Korea) and supported by the Technological Innovation R&D Program (S2829590) funded by the Small and Medium Business Administration (SMBA, Korea).

## REFERENCES

1. J. A. Palacios and R. Ganesan, *Compos. Part B-Eng.*, **166**, 497 (2019).
2. F. L. Jin, R. R. Hu and S. J. Park, *Compos. Part B-Eng.*, **164**, 287 (2019).
3. A. S. Hicyilmaz, Y. Altin and A. Bedeloglu, *J. Appl. Polym. Sci.*, **136**, 47616 (2019).
4. M. Shabbir, L. J. Rather and F. Mohammad, *Ind. Crop. Prod.*, **119**, 277 (2018).
5. M. M. Hassan, *Colloids Surf. A*, **582**, 123819 (2019).
6. D. Kim, *Korean J. Chem. Eng.*, **35**, 1680 (2018).
7. X. W. Cheng, J. P. Guan, X. H. Yang, R. C. Tang and F. Yao, *J. Clean. Prod.*, **223**, 342 (2019).
8. X. W. Cheng, J. P. Guan, X. H. Yang and R. C. Tang, *Thermochim. Acta*, **665**, 28 (2018).
9. X. W. Cheng, R. C. Tang, F. Yao and X. H. Yang, *Prog. Org. Coat.*, **132**, 936 (2019).
10. Y. W. Wang, R. Shen, Q. Wang and Y. Vasquez, *ACS Omega*, **3**, 6330 (2018).
11. A. Castellano, C. Colleoni, G. Iacono, A. Mezzi, M. R. Plutino, G. Malucelli and G. Rosace, *Polym. Degrad. Stabil.*, **162**, 148 (2019).
12. X. W. Cheng, J. P. Guana, P. Kiekens, X. H. Yang and R. C. Tang, *React. Funct. Polym.*, **134**, 58 (2019).
13. R. Haji, B. Otazaghine, R. Sonnier, R. E. Hage, S. Rouif, M. Nakhil and J. M. Lopez-Guesta, *Polym. Degrad. Stabil.*, **166**, 86 (2019).
14. M. Barbalini, M. Bartoli, A. Tagliaferro and G. Malucelli, *Polymers*, **12**, 811 (2020).
15. I. Joradanov, E. Magovac, A. Fahami, S. Lazar, T. Kolibaba, R. J. Smith, S. Bischof and J. C. Grunlan, *Polym. Degrad. Stabil.*, **170**, 108998 (2019).
16. T. Nosaka, R. Lankone, P. Westerhoff and P. Herckes, *Polym. Test.*, **86**, 106497 (2020).
17. H. J. Xu, F. L. Jin and S. J. Park, *B. Korean Chem. Soc.*, **30**(11), 2643 (2009).
18. M. J. Oh and P. J. Yoo, *Korean J. Chem. Eng.*, **37**, 189 (2020).
19. G. Malucelli, *Coatings*, **10**, 333 (2020).
20. G. Mourgas, E. Giebel, T. Schneck, J. Unold and M. R. Buchmeiser, *J. Appl. Polym. Sci.*, **136**, 47829 (2019).
21. X. W. Cheng, J. P. Guan, X. H. Yang, R. C. Tang and Y. Fan, *J. Mater. Res. Technol.*, **9**, 700 (2020).
22. H. Vothi, C. Nguyen, L. H. Pham, D. Q. Hoan and J. Kim, *ACS Omega*, **4**, 17791 (2019).
23. Z. Chi, Z. Guo, Z. Xu, M. Zhang, M. Li, L. Shang and Y. Ao, *Polym. Degrad. Stabil.*, **176**, 109151 (2020).
24. S. Zhu, W. Gong, J. Luo, X. Meng, Z. Xin, J. Wu and Z. Jiang, *Polymers*, **11**, 1304 (2019).
25. E. Kaynak, M. E. Üreyen and A. S. Koparal, *Mater. Today Proc.*, **31**, S258 (2020).
26. P. Mathur, J. N. Sheikh and K. Sen, *Polym. Degrad. Stabil.*, **174**, 109101 (2020).
27. G. Shan, L. Jia, T. Zhao, C. Jin, R. Liu and Y. Xiao, *Fiber. Polym.*, **18**, 2196 (2017).
28. Q. Li, Y. Chen, X. Song, Y. Xie, Q. Hou and G. Shi, *J. Appl. Polym. Sci.*, **132**, 41677 (2015).
29. Z. Jiang, H. Li, Y. He, Y. Liu, C. Dong and P. Zhu, *Appl. Surf. Sci.*, **479**, 765 (2019).
30. T. Zhou, H. Xu, L. Cai and J. Wang, *Appl. Surf. Sci.*, **507**, 14575 (2020).
31. X. Wang, M. Xu, Z. Zhang, Y. Leng and B. Li, *J. Anal. Appl. Pyrol.*, **134**, 243 (2018).
32. X. Hu, H. Yang, Y. Jiang, H. He, H. Liu, H. Huang and C. Wan, *J. Hazard. Mater.*, **379**, 120793 (2019).
33. P. Tian, Y. Lu, D. Wang, G. Zhang and F. Zhang, *Polym. Degrad. Stabil.*, **165**, 220 (2019).
34. S. Huang, L. Zhong, S. Li, M. Liu, Z. Zhang, F. Zhang and G. Zhang, *Cellulose*, **26**, 2715 (2019).
35. Z. Du, B. Ji and K. Yan, *J. Clean. Prod.*, **183**, 810 (2018).
36. J. Lv, Q. Zhou, G. Liu, D. Gao and C. Wang, *Carbohydr. Polym.*, **113**, 344 (2014).
37. Z. Jiang, D. Xu, X. Ma, J. Liu and P. Zhu, *Cellulose*, **26**, 5783 (2019).

38. F. L. Jin, C. L. Ma, B. T. Guo and S. J. Park, *B. Korean Chem. Soc.*, **40**(10), 991 (2019).
39. S. S. Yao, Q. Q. Pang, R. Song, F. L. Jin and S. J. Park, *Macromol. Res.*, **24**(11), 961 (2016).
40. W. Jiang, F. L. Jin and S. J. Park, *J. Ind. Eng. Chem.*, **27**(1), 40 (2015).
41. F. M. Bezerra, Ó. G. Carmona, C. G. Carmona, A. M. S. Plath and M. Lis, *Process Biochem.*, **77**, 151 (2019).
42. S. Huang, Y. Feng, S. Li, Y. Zhou, F. Zhang and G. Zhang, *Polym. Degrad. Stab.*, **164**, 157 (2019).
43. S. Li, L. Zhong, S. Huang, D. Wang, F. Zhang and G. Zhang, *Polym. Degrad. Stab.*, **164**, 145 (2019).
44. R. Qin, Y. Song, M. Niu, B. Xue and L. Liu, *Polym. Degrad. Stab.*, **171**, 109028 (2020).
45. Y. Pan, L. Liu, Y. Zhang, L. Song, Y. Hu, S. Jiang and H. Zhao, *Carbohydr. Polym.*, **206**, 396 (2019).
46. C. Ling and L. Guo, *Carbohydr. Polym.*, **230**, 115648 (2020).
47. Y. Fang, X. Liu and X. Tao, *Prog. Org. Coat.*, **134**, 162 (2019).
48. Z. Lv, Y. T. Hu, J. P. Guan, R. C. Tang and G. Q. Chen, *Mater. Lett.*, **241**, 136 (2019).
49. F. Hao, W. Geng, Q. Liu, W. Dong, F. L. Jin and S. J. Park, *B. Mater. Sci.*, **42**, 216 (2019).
50. S. Huo, J. Wang, S. Yang, B. Zhang, X. Chen, Q. Wu and L. Yang, *Polym. Degrad. Stab.*, **146**, 250 (2017).
51. G. Yang, W. H. Wu, Y. H. Wang, Y. H. Jiao, L. Y. Lu, H. Q. Qu and X. Y. Qin, *J. Hazard. Mater.*, **366**, 78 (2019).
52. Y. Pan, L. Liu, L. Song, Y. Hu, W. Wang and H. Zhao, *Polym. Degrad. Stab.*, **165**, 145 (2019).
53. T. Chen, J. Hong, C. Peng, G. Chen, C. Yuan, Y. Xu, B. Zeng and L. Dai, *Carbohydr. Polym.*, **208**, 14 (2019).